

Biomacromorecures. Tradior manascript, available in 11410 2012 December

Published in final edited form as:

Biomacromolecules. 2011 December 12; 12(12): 4204-4212. doi:10.1021/bm200975a.

Protein and Mineral Composition of Osteogenic Extracellular Matrix Constructs Generated with a Flow Perfusion Bioreactor

Richard A. Thibault^a, **Antonios G. Mikos**^a, and **F. Kurtis Kasper**^{a,*}
^aDepartment of Bioengineering Rice University P.O. Box 1892, MS-142 Houston, TX 77251-1892

Abstract

This study investigated the temporal composition of an osteogenic extracellular matrix construct generated by culturing mesenchymal stem cells in an electrospun biodegradable poly(\varepsilon-caprolactone) fiber mesh scaffold within a flow perfusion bioreactor. Constructs of different extracellular matrix maturities were analyzed for their protein and mineral composition at several culture durations by liquid chromatography-tandem mass spectroscopy, scanning electron microscopy, energy dispersive x-ray diffraction, x-ray diffraction, and calcium and phosphate assays. The analysis revealed that at short culture durations the cells deposited cellular adhesion proteins as a prerequisite protein network for further bone formation. At the later culture durations, the extracellular matrix was composed of collagen 1, hydroxyapatite, matrix remodeling proteins, and regulatory proteins. These results suggest that the later culture duration constructs would allow for improved bone regeneration due to the ability to mineralize and the capabilities for future remodeling.

Keywords

osteogenic; MSC; proteomics; hydroxyapatite; flow perfusion bioreactor

Introduction

Bone defects can arise from a variety of sources, including trauma, resection of tumors, and congenital disorders. Autograft bone stands as the gold standard material for reconstruction of the missing bony tissue, due to its ability to integrate with the surrounding bone and to grow with the patient. However, autograft bone is of limited availability and may present an associated donor site morbidity. Bone tissue engineering seeks to develop alternative materials to overcome the limitations of bone grafts by providing a supporting environment and incorporating bioactive and biomimetic domains found in mature bone to induce bone formation and regeneration.

The organic phase of the extracellular matrix (ECM) of mature bone is composed largely of collagen 1, while the mineral component consists of hydroxyapatite.⁵ Other proteins such as collagen 5, fibril-associated collagens, proteoglycans, glycoproteins, growth factors, and matrix metalloproteinases (MMPs) are present in minor quantities, but are also important components of the composition of bone.⁵ Collagen 5 and the fibril-associated collagens help regulate the correct fibril diameter of collagen 1 in the tissue. The proteoglycans and glycoproteins bind to growth factors, nucleate hydroxyapatite deposition, and facilitate bone

cell attachment. Select growth factors promote osteoblast infiltration and blood vessel ingrowth into the bone, while the MMPs allow for the remodeling of bone.

Many bone tissue engineering scaffolds have been designed incorporating domains that mimic the varied components, structures, and bioactive nature of mature bone. Examples include, prefabricated polymers also containing collagen with deposited apatite crystals, calcium phosphate cements with growth factor releasing microspheres, and gelatin hydrogels with adsorbed or absorbed growth factors.^{6–10} In our laboratory, we have investigated an osteogenic tissue engineered construct, comprising an electrospun poly(ε-caprolactone) (PCL) scaffold and an ECM coating generated by osteogenically differentiated mesenchymal stem cells (MSCs) cultured for 12 days within a flow perfusion bioreactor (PCL/ECM constructs).^{11,12} We have demonstrated that osteogenically predifferentiated MSCs cultured on acellular PCL/ECM constructs retained their differentiation without the presence of osteogenic cell culture supplements.^{11,12} Moreover, these acellular PCL/ECM constructs supported continued mineralization in culture medium.¹² These constructs were shown to contain the major bone components: collagens, glycosaminoglycans, and a calcium-bearing mineral.^{13,14}

In this study, we hypothesize that the ECM deposited by MSCs within the constructs cultured under flow perfusion conditions replicates the proteins and minerals found in mature bone and that there is a temporal effect in the deposition of these components during *in vitro* culture. To test these hypotheses, we analyzed the protein and mineral compositions of *in vitro* MSC-generated ECM constructs at different culture durations after a decellularization and drying procedure. Electrospun PCL scaffolds were seeded with osteogenically pre-differentiated MSCs and cultured within a flow perfusion bioreactor for 8, 12, and 16 days in osteogenic differentiation medium. Day 12 constructs were decellularized, dried, sterilized, reseeded with fresh pre-differentiated MSCs, and cultured in osteogenic medium within a flow perfusion bioreactor for an additional 4, 8, and 16 days. Each construct group was decellularized and air dried prior to imaging with scanning electron microscopy (SEM), protein analysis with liquid chromatography-tandem mass spectroscopy (LC-MS/MS), and mineral analysis with energy dispersive x-ray diffraction (EDX), x-ray diffraction (XRD), calcium assay, and phosphate assay.

Materials and Methods

Fabrication of PCL Scaffolds

PCL with an inherent viscosity of 0.68 dL/g, number average molecular weight of 61000 \pm 2500 Da, and a weight average molecular weight of 88500 \pm 2700 Da (DURECT Corporation, Pelham, AL) was dissolved in a 5:1 (vol/vol) chloroform:methanol solution at 22 wt% (wt/wt). The PCL solution was electrospun as previously described to produce fiber mesh mats with a porosity of 84% and an average fiber diameter of approximately 5 μm , from which disc-shaped scaffolds 8 mm in diameter and approximately 1 mm thick were prepared using a biopsy punch. 15 The scaffolds were then sterilized by exposure to ethylene oxide (Andersen Sterilizers Inc., Haw River, NC) for 14 hours and pre-wetted using an ethanol gradient one hour prior to cell seeding.

MSC Isolation

MSCs were harvested and pooled from the marrow of tibiae and femora of 4 male Fischer 344 rats (150 - 175 g; Charles River Laboratories, Wilmington, MA) per isolation procedure as previously described. Care of the rats in this study was in accordance with a protocol approved by the Rice University Institutional Animal Care and Use Committee. The MSCs were cultured in complete osteogenic media (α -MEM (Invitrogen, Carlsbad, CA), 10% FBS

(Gemini Bio-Products, West Sacramento, CA), 10 mM β -glycerol-2-phosphate, 10 nM dexamethasone, 50 μ g/mL ascorbic acid, 50 μ g/mL gentamicin, 100 μ g/mL ampicillin, and 0.5 μ g/mL fungizone (all from Sigma-Aldrich, St. Louis, MO)) for 7 days to predifferentiate them along the osteogenic pathway. ¹⁶ Rat femora from select MSC isolations were cleaned of soft tissues and retained frozen in Millipore-filtered water for later mineral content analysis.

MSC Culture on PCL Scaffolds

Prior to cell seeding, seventy-eight pre-wetted PCL scaffolds were transferred into complete osteogenic medium for 2 hours, press-fit into cassettes, and maintained briefly in an incubator. A quarter-million of the isolated MSCs in 200 μL of complete osteogenic medium were seeded onto each PCL scaffold, and the MSCs were allowed to adhere to the scaffold overnight in the incubator. Subsequently, the scaffold-containing cassettes were placed into a flow perfusion bioreactor at a flow rate of 1 mL/min with 200 mL of complete osteogenic medium per bioreactor, which was exchanged every 2 days. 17 Twelve constructs each were removed from the bioreactors at day 8 (PCL day 8) and day 16 (PCL day 16), while a total of fifty-four constructs were removed at day 12 (PCL day 12). The MSCs that generated the osteogenic ECM in the PCL scaffolds *in vitro* were then removed by a decellularization process, which involved 3 cycles of freezing in liquid N_2 and thawing in a 37°C water bath, followed by 10 min. of ultrasonication. Forty-two of the day 12 constructs previously generated were aseptically air dried and sterilized for 14 hours in ethylene oxide (PCL/ECM constructs). Six of the day 12 constructs (PCL/ECM 0) were retained for LC-MS/MS analysis as a control for the remaining PCL/ECM constructs.

MSC Culture on PCL/ECM Constructs

Prior to seeding with fresh MSCs, acellular PCL/ECM constructs were transferred to complete osteogenic media for 2 hours, press-fit into cassettes, and maintained briefly in the incubator. MSCs were seeded and cultured on the constructs as described in the previous section. Twelve constructs each were removed from the bioreactors at day 4 (PCL/ECM day 4), day 8 (PCL/ECM day 8), and day 16 (PCL/ECM day 16), and the reseeded MSCs were removed by the decellularization procedure described in the previous section.

Protein Extraction

Six constructs from each group were combined and minced with microscissors, then placed in 1.5 mL of 7 M urea buffer (7 M urea, 2 mM sodium EDTA, 50 mM tris(hydroxymethyl)amino-methane, 0.5% triton X-100, 1% protease inhibitor cocktail, 2 mM dithiothreitol, 1 mM phenylmethylsulfonyl fluoride (all from Sigma-Aldrich)) and rotated at 4°C overnight. The solution was strained to remove PCL fragments, centrifuged at 2000 rpm for 10 min. to pellet the mineral components, and the supernatant containing the protein extract was aliquoted into two 750 μ L samples and frozen at -20°C.

LC-MS/MS Analysis

One of the frozen 750 µL supernatant samples from each group was defrosted and analyzed at the proteomics core facility at M.D. Anderson Cancer Center via LC-MS/MS according to their standard operating procedure. Briefly, the protein solutions were precipitated using an equal volume of 3.9 M ammonium sulfate and centrifuged at 13000 rpm for 30 min. at 4°C. The pellet was resuspended in Rapidgest (Waters, Milford, Massachusetts) containing trypsin and 50 mM sodium bicarbonate, incubated overnight at 37°C, and subsequently injected into a liquid chromatography column connected to a tandem mass spectrometer (LC-MS/MS). The resulting spectra, excluding the peaks from human keratin and bovine trypsin, were analyzed using the Mascot search engine. ¹⁸ Search parameters were limited to

the Rattus taxonomy (66908 sequences) and with the trioxidation of cysteine and oxidation of methionines as a variable modification. Peptide mass tolerances were set to 2 Daltons, fragment mass tolerances were set to 1 Dalton, and two missed cleavages were accepted. Searches were performed using the non-redundant proteins at the National Center for Biotechnology Information (NCBInr version 20100908 (11756863 sequences, 4014994744 residues)). Protein hits were scored using standard Mascot scoring and a Mascot score greater than 30 was regarded as significant (p<0.05). An exponentially modified Protein Abundance Index (emPAI) score for each protein hit was also determined by the software. The emPAI score is roughly correlated to protein concentration and can be used for relative quantitation. ¹⁹ Manual analysis of the protein hit list was used to identify the ECM proteins present within each group.

Calcium and Phosphate Assays

Three constructs from each group were rinsed twice with sterile Millipore-filtered water, and 1 mL of 1 N acetic acid was added to each construct. The constructs were minced with microscissors and placed on a shaker table at room temperature for 1 day at 75 rpm to dissolve any mineral salts present in the construct. Three femora were fragmented with a mortar and pestle and placed into 1 mL of 12 N hydrochloric acid overnight at room temperature. The calcium content of the constructs and bones were determined as previously described, with each sample measured in triplicate. ¹² The phosphate content of the constructs and bones was measured in triplicate and was determined by following the protocol supplied by the manufacturer of the assay kit (R & D Systems, Minneapolis, MN).

SEM and EDX Analysis

Femora fragments and one construct from each group were fixed with 2.5% glutaraldehyde solution (Sigma-Aldrich) at room temperature for 45 min., dried using an ethanol gradient, frozen, and then lyophilized. The bone fragments and constructs were sputter coated with gold prior to imaging with an FEI Quanta 400 ESEM FEG (FEI Company, Hillsboro, OR) at 1000x magnification in the center of each sample. Additionally, each specimen was scanned at 1000x magnification at three different spots using an EDX (EDAX Inc., Mahwah, NJ) integrated with the SEM until the relative intensities of the peaks became stable, and the resulting peaks were identified using the EDAX Genesis software package (EDAX Inc.). Each element identified was quantified into an atomic percentage by the EDAX software, and the Ca:P ratio was determined by dividing the calcium percentage by the phosphorous percentage.

XRD Analysis

The mineral pellets for each group, isolated during the protein extraction step, were washed twice with Millipore-filtered water to remove soluble salts remaining in the pellet and subsequently air dried. Femora fragments were crushed into a fine powder using a ceramic mill. The powder from each group was placed on a zero background wafer (Rigaku, The Woodlands, TX) and analyzed using a D/Max XRD (Rigaku). The powders were scanned for a fixed time of 12 seconds per step from 10° to 60° using a 2 mm divergent slit, a step size of 0.10° , and a variable receiving slit. Spectrum identification was performed using Jade 9 software (MDI, Livermore, CA) and matched with crystals from the PDF 4 database provided with the Jade 9 software using a chemistry filter for compounds containing only calcium, phosphorous, oxygen, and carbon. The spectra were matched according to best figure of merit and a 20 offset between -0.100 and 0.100, and any peaks not accounted for by the first identification procedure were matched with the same database. The percent crystallinity was determined by adding a linear background, manually identifying peaks, and fitting the peak profiles to the spectra until the residual stabilized. This procedure was repeated three times and the resulting crystallinities were averaged.

Statistical Analysis

Results are presented as means \pm standard deviations. Statistical significance for the calcium and phosphate assay data was determined using Tukey's Honestly Significant Differences test with a 95% or a 99% confidence interval with JMP IN 5.1 software (SAS Institute Inc., Cary, NC).

Results

LC-MS/MS Analysis

No ECM proteins were detected by LC-MS/MS analysis for the PCL day 8 constructs (Table 1). The PCL day 12 constructs were found to contain fibronectin, a cell binding protein that forms a fibrillar network extending between adjacent cells; fibulin-1, a protein that binds to fibronectin and regulates its fibril diameter; procollagen 6, a cell binding protein that interacts with fibronectin and collagen 1 and is suggested to anchor the basement membrane to underlying connective tissue; periostin, a protein that plays a role in the formation of collagen cross-links, interacts with fibronectin, and directly binds to bone morphogenic protein-1 (BMP-1); collagen 1, the main structural protein of bone; and MMP-2, a gelatinase that may play a role in angiogenesis by remodeling the ECM.^{5,20–24} The emPAI score for fibronectin was higher than for collagen 1, periostin, procollagen 6, and MMP-2 in the PCL day 12 constructs, and no score was reported for fibulin-1.

The PCL day 16 constructs were found to retain all proteins observed in the PCL day 12 constructs, with the exception of fibulin-1, based on LC-MS/MS analysis. Three additional proteins were found within the constructs, including: high-temperature requirement A serine peptidase 1 (HtrA1), a peptidase that degrades fibronectin and inhibits transforming growth factor- β (TGF- β)/BMP signaling; thrombospondin 2 (TSP-2), a protein that inhibits angiogenesis and binds to fibronectin; and pigment epithelium-derived factor (PEDF), another protein that inhibits angiogenesis, expressed during early bone development, and may counteract vascular endothelial growth factor A (VEGF-A). The emPAI score was higher for fibronectin than for all other proteins detected in the PCL day 16 constructs, with the exception of TSP-2, which reported no score.

The PCL/ECM 0 constructs were found by LC-MS/MS to contain fibronectin, fibulin-1, HtrA1, collagen 1, procollagen 6, and thrombospondin 1 (TSP-1), a protein that inhibits angiogenesis, activates the TGF β family of proteins, and binds to glycosaminoglycans. The emPAI score for HtrA1 was higher than for all other proteins detected in the PCL/ECM 0 constructs.

LC-MS/MS detected the presence of two ECM proteins in the PCL/ECM day 4 constructs: osteopontin, a calcium-binding glycoprotein that binds cells and preferentially accumulates at ECM discontinuities including healing bone surfaces and at cell-matrix interfaces, such as on activated bone surfaces; and secreted phosphoprotein 2, 24 kDa (SPP-24 or SPP-2), a protein that binds BMP-2 and hydroxyapatite, and regulates the bioavailability of BMP-2. ^{29,30} Within these constructs, osteopontin presented a higher emPAI score than SPP-24.

LC-MS/MS analysis of the PCL/ECM day 8 constructs detected periostin at a higher level than procollagen 6 (as reflected by the emPAI scores), while osteopontin and SPP-24 were no longer present. The PCL/ECM day 16 constructs contained procollagen 6, fibronectin, and PEDF along with fibulin-1 and alkaline phosphatase, an enzyme that hydrolyzes pyrophosphates and is an early marker of osteogenic differentiation. The emPAI scores for procollagen 6 and fibulin-1 were higher than the scores for alkaline phosphatase, PEDF, and fibronectin.

Calcium and Phosphate Assays

The number of moles of calcium ions and phosphate ions present in the constructs was found to increase with increasing culture durations (Figure 1). The PCL day 8 and PCL day 12 constructs demonstrated a significantly lower (p<0.05) amount of calcium ions present as compared to PCL/ECM day 16 constructs. The PCL day 8 constructs also exhibited a significantly lower (p<0.05) amount of calcium ions as compared to the PCL/ECM day 8 constructs. In addition, the PCL day 8 constructs were observed to have a significantly lower (p<0.05) amount of phosphate ions as compared to PCL/ECM day 16 constructs. The ratio of calcium to phosphorous (Ca:P) as determined by the calcium and phosphate assays for each group is illustrated in Table 2. The Ca:P ratio for PCL day 12 constructs was significantly lower (p<0.01) than that of mature bone, when using the calcium and phosphate assay results. Additionally, the Ca:P ratio for the PCL day 16, PCL/ECM day 4, PCL/ECM day 8, and PCL/ECM day 16 constructs were significantly lower (p<0.05) than that of mature bone, when using the calcium and phosphate assay results.

Scanning Electron Microscopy

Nodules were found by SEM to be present on the constructs, and the abundance of nodules was found qualitatively to increase with increasing culture durations (Figure 2). PCL day 8 constructs demonstrated sparse nodules with a matrix coating on the electrospun PCL, whereas PCL day 16 constructs showed large amounts of nodules present on top of the matrix coating. PCL/ECM day 8 and PCL/ECM day 16 constructs demonstrated a full coating of nodules on the surface.

Electron Dispersive X-ray Spectroscopy

The EDX spectrum in Figure 3 illustrates that the PCL day 16 constructs had carbon, oxygen, phosphorous, calcium and gold atoms present. The gold atoms were an artifact related to the gold coating necessary for SEM imaging. The ratio of calcium to phosphorous (Ca:P), as calculated from the atomic percentage data obtained from the EDAX software in the EDX analysis, of the entire scanned region seen in the SEM micrographs in Figure 2 is presented in Table 2.

X-Ray Diffraction Analysis

The XRD spectra of the various groups are illustrated in Figure 4. As the ECM matured for each of the PCL and PCL/ECM based constructs, there was an increase in intensity of the peaks at 2θ angles of 26°, 28°, 32°, 40°, and 50° and a slight decrease of the peak at 21°. The analysis demonstrated that all constructs had a major phase composed of hydroxyapatite (HAp) and a minor phase composed of tricalcium phosphate (TCP), except for the PCL day 8 constructs (Table 3). Each construct demonstrated crystallinities over 80%, with the exception of the PCL day 8 construct. The figures of merit for all groups were large, which indicated a poor fit of the spectra of the mineral content of the constructs to the database values for pure HAp and TCP. However, the 2θ offset, which represents how much the software had to shift the peaks to match the HAp and TCP spectra within the database, was nil for some constructs, including PCL day 12 HAp, PCL/ECM day 4 HAp, PCL/ECM day 8 TCP, and mature bone HAp. The software was unable to match the minerals from the PCL day 8 constructs to any of the compounds in the database that contained the elements found by EDX analysis and was unable to determine the percent crystallinity.

Discussion

Prior analyses of constructs developed within our laboratory have demonstrated that the *in vitro*-generated ECM deposited by MSCs onto PCL and titanium constructs promoted

osteogenic differentiation of MSCs *in vitro* and that the titanium-based constructs comprised collagens, glycosaminoglycans, and a calcium-based mineral.^{12,13} The goal of this study was to determine whether the ECM deposited by MSCs within the constructs cultured under flow perfusion conditions replicates the proteins and minerals found in mature bone and if there is a temporal effect in the deposition of these components during *in vitro* culture.

For the PCL day 8 constructs no secreted proteins were detected by LC-MS/MS. However, an extracellular matrix coating appeared to be present via SEM for these constructs. The lack of detected protein via LC-MS/MS may reflect that the amount of protein extracted from the constructs was below the threshold for detection.

For the PCL day 12 constructs, a high abundance of fibronectin was observed, which may facilitate cell adhesion to the PCL scaffold. Further, fibulin-1 was detected within the PCL day 12 constructs. Fibulin-1 is known to regulate the fibril diameter of fibronectin and may reflect that the fibronectin was in a fibrillar form. However, an emPAI score for fibulin-1 was not generated, which suggests that the protein was a weak hit and may not be present within the constructs. The presence of secreted collagen 1 and periostin within the constructs suggests the production of a collagenous network by the cells, as periostin plays a role in cross-linking collagen. Also, the presence of procollagen 6 in similar quantities to collagen 1 may reflect that it was deposited to assist in anchoring the collagen 1 network to the deposited fibronectin within the construct. MMP-2 was observed in similar quantities to collagen 1, which may suggest that the MSCs secreted the protease so that it would be able to degrade any malformed collagen that may have been deposited.

For the PCL day 16 constructs, high levels of fibronectin remained present within the constructs. A slight decrease in procollagen 6 as compared to the PCL day 12 constructs was also observed. However, there were similar amounts of collagen 1, MMP-2, and periostin in PCL day 12 and PCL day 16 constructs. The loss of fibulin-1 may be explained by the appearance of TSP-2, which binds to fibronectin as well. However, similar to fibulin-1, the emPAI score was not given for TSP-2 and thus it may not be present within the constructs. The decrease in fibronectin may suggest that HtrA1 degraded some of the deposited fibronectin. A decrease in procollagen 6 may also be linked to the decrease in fibronectin, since it is a linker protein between collagen 1 and fibronectin. The appearance of PEDF and TSP-2 may suggest that the MSCs were beginning the mineralization process of the constructs. PEDF and TSP-2 are known to bind to collagen 1, found in developing bone matrix, and PEDF is secreted at high levels by osteoblasts, while TSP-2 is secreted by MSCs undergoing osteogenic differentiation. ^{27,32–34} In addition, TSP-2 and PEDF are antiangiogenic factors, thus their presence may imply that the MSCs are regulating an angiogenic factor, such as VEGF-A or bFGF.

With respect to the PCL/ECM day 4 constructs, both osteopontin and SPP-24 were observed with high emPAI scores. SPP-24 is found at high levels in the bones of neonates and may be important in neonatal skeletal development and the acquisition of peak bone mass. The presence of both osteopontin and SPP-24 may reflect that the reseeded MSCs recognized the PCL/ECM scaffold as a bony surface and were depositing proteins that encouraged cell adhesion to the surface.

For the PCL/ECM day 8 constructs, the disappearance of both osteopontin and SPP-24 may imply that the proteins have performed their function of recruiting more cells to the damaged bony surface and were not necessary for further development. With the deposition of procollagen 6 and periostin, it appears that the MSCs were developing the pre-requisite matrix for further mineralization of the constructs.

Regarding the PCL/ECM day 16 constructs, the presence of procollagen 6, fibulin-1, and fibronectin suggests that the MSCs are further developing the extracellular matrix. The disappearance of periostin may be due to batch differences between the MSCs used for generation of the scaffold. The secretion of alkaline phosphatase indicates that the MSCs were undergoing osteogenic differentiation inducing further mineralization of the constructs. The deposition of PEDF also signifies that the MSCs had fully differentiated into osteoblasts.

Of interest is the fact that there were no similar proteins observed between the PCL/ECM day 4 and either the PCL day 12 or the PCL/ECM 0 constructs. This is surprising since the PCL/ECM day 4 constructs were derived from MSCs cultured for 4 days on sterilized, dried, and decellularized PCL day 12 constructs (i.e., PCL/ECM 0 constructs). However, the PCL day 12 constructs were not sterilized prior to analysis. Consequently, the PCL/ECM 0 constructs provide a baseline for comparison, as they were prepared in the same manner as the PCL day 12 constructs, with the exception that the PCL/ECM 0 constructs were sterilized via exposure to ethylene oxide prior to matrix analysis.

Similar proteins were found to be present in the PCL 12 and PCL/ECM 0 constructs, based on LC-MS/MS analysis, as expected. Specifically, fibronectin, fibulin-1, collagen 1, and procollagen 6 were detected in both constructs. However, HtrA1 and thrombospondin 1 were measured in the PCL/ECM 0 construct, while MMP-2 and periostin were not detected. The difference may reflect slight variability between the batches of MSCs used to generate the constructs or limitations of the LC-MS/MS technique itself, but it does not appear to indicate a detrimental effect of the sterilization procedure on the matrix, as characterized by LC-MS/MS. Interestingly, the PCL/ECM 4 scaffolds did not retain any of the proteins detected in the PCL/ECM 0 scaffolds. The MSCs seeded onto the PCL/ECM 0 constructs may have degraded the proteins present, which by day 4 of culture (PCL/ECM day 4) could have been below the threshold level for detection.

The protein compositions of the constructs as measured by LC-MS/MS in the present study did not fully resemble the composition of mature or developing bone. However, the constructs began to consist of several of the mature bone proteins as culture duration increased. Mature and developing bone is composed of collagen 1, fibronectin, glycosaminoglycan substituted proteoglycans such as decorin and biglycan, MMPs such as MMP-2 and MMP-9, and growth factors such as BMP-2, VEGF, and basic fibroblast growth factor (bFGF).⁵ From our prior studies, collagen 1 and some glycosaminoglycans (GAGs) were expected. However, no GAG substituted proteoglycans were detected in any of the constructs and this may be due to the amount of proteoglycans extracted being below the threshold of LC-MS/MS detection. Alternatively, the lack of detected proteoglycans and GAGs may be due to the lack of deglycosylation and chondroitinase treatment of the protein extract.

The appearance of growth factors may be expected within the constructs, nevertheless, only the anti-angiogenic growth factor PEDF was reported. The lack of detection of VEGF-A is not unexpected due to its high diffusivity and its lack in ability to bind to ECM molecules when it is present in its shortest splice form. As well, bFGF has a short half-life *in vivo* and washes easily away if it is not bound to heparan sulfate. Furthermore, the lack of VEGF-A or bFGF may be due to a low amount of it being secreted by the MSCs, thus it would not be detected by the LC-MS/MS technique. However, the lack of detection of TGF β -1 and BMP-2 was unexpected. Both TGF β -1 and BMP-2 encourage bone formation and may be expected to be secreted by the MSCs, especially in the PCL/ECM based scaffolds since they resemble bone to a higher degree than the PCL scaffolds. However, these growth factors, although absent in the present analyses, may appear at longer culture

durations or the extracted amount may be below the detection level of the LC-MS/MS. Indeed, previous studies employing immunohistochemistry analysis of matrix produced by MSCs cultured under flow perfusion conditions on scaffolds comprising a blend of starch and PCL were found to contain several bone-related growth factors, including TGF β -1, fibroblast growth fator-2, VEGF and BMP-2. As none of these growth factors were detected by LC-MS/MS in the present study, the protein extraction procedure or the sensitivity of the LC-MS/MS technique may not have been sufficient for full characterization of the protein component of ECM constructs of the dimensions explored in this study.

The mineral component of the constructs was demonstrated to contain Ca^{2+} and $\text{PO}_4{}^{3-}$ ions, and the amount of these ions increased over time. The increase in Ca^{2+} is similar to what has been previously observed in bioreactor studies using titanium and PCL fiber mesh scaffolds in our laboratory. 12,13,40 It can also be seen through the Ca:P ratio that the concentration of the Ca^{2+} and $\text{PO}_4{}^{3-}$ ions was very similar to each other at each culture period, excluding the case of the PCL day 8 constructs. Comparing to the ratio found in mature bone, it can be seen that the ratio was almost double what is found in the constructs. The difference may be accounted for by the method of generating the constructs, which may leave DNA fragments and cell debris throughout the constructs. These cellular remnants are potential sources of $\text{PO}_4{}^{3-}$, and may skew the Ca:P ratio towards a lower value.

The EDX spectrum in Figure 3 demonstrated that the constructs were composed of carbon, oxygen, phosphorous, and calcium. Comparing the EDX spectrum from PCL day 8 constructs to PCL day 16 constructs (data not shown), there was a noticeably lower intensity for the calcium and phosphorous peaks in the PCL day 8 constructs. Combined with a lower visible number of nodules in the SEM micrograph of the PCL day 8 construct, this implies that the nodules are the main source of the calcium and phosphorous peaks seen in the EDX spectra of all the constructs. However, in the absence of a more detailed analysis, the nodules cannot be irreproachably shown to be the mineral deposits found within the constructs.

Table 2 shows the calculated Ca:P ratio from the EDS spectra and demonstrates that the Ca:P ratio of all the constructs, excluding the PCL day 8 and PCL/ECM day 8 constructs, was similar to mature bone. From the ratios, it can be seen that the minerals are not pure HAp, which has a ratio of 1.67. However, the HAp present in bone has many substitutes including Na⁺, Mg²⁺, HPO₄²⁻, CO₃²⁻, OH⁻, Cl⁻, and F⁻, thus an observed ratio within the range of 1.41 to 1.99 would not be unexpected.⁴¹ The observed Ca:P ratios in the constructs and bone also suggest that the minerals could be amorphous calcium phosphate (ACP), due to the varied stoichiometry of ACP, octacalcium phosphate (OCP), or a mixture of several mineral phases.^{41,42} However, combining the Ca:P ratio with the analysis of the XRD spectra suggests that the minerals were a mixture of two phases, composed mainly of HAp with a minor phase of TCP present, with the exception of the PCL day 8 constructs.

Nevertheless, the analysis of the minerals may have been affected by the decellularization procedure and isolation of the mineral pellets from the constructs. The decellularization procedure requires multiple freeze and thaw steps in water and a drying step, while the isolation of the mineral pellets required a water wash step to remove any remnant protein extract solution and a subsequent drying step. The water wash and drying steps may have dissolved amorphous mineral components or altered the crystallinity of the minerals. However, all samples for the various mineral analyses were treated in the same fashion, thus any changes that may have occurred would be consistent across samples.

The peak locations and breadths visible in the XRD spectra for PCL day 16 and PCL/ECM day 16 constructs and the Ca:P ratios derived from the EDX spectra of both of these constructs were similar to that of the mature bone. The spectra of both of these constructs developed broad and minor peaks at 28°, 40°, and 50°, similar to that seen in the spectrum of mature bone and, with the increase in intensity of the major peaks at 26° and 32° as the constructs increased in culture duration, suggests that the mineral composition is approaching that of mature bone. Additionally, the figure of merits of each mineral type in the construct approached 0 and there was a trend of increasing crystallinity that approached that of mature bone as the culture duration increased.

It can also be observed that the spectrum of PCL day 16 constructs rather than that of PCL/ECM day 4 constructs had a greater resemblance to mature bone, although both constructs were cultured for the same length of time. This may be because the scaffolding for the PCL/ECM based constructs was based on the PCL day 12 constructs. As can be seen, the spectrum of the PCL/ECM day 4 constructs appears to resemble that of the PCL day 12 constructs. The reseeding procedure covers the surface of the decellularized PCL day 12 constructs with MSCs, and osteopontin deposited by the MSCs may have prevented the maturation of the previously deposited minerals. However, the maturation of the minerals may have also been affected by the decellularization procedure or by the reseeding of the pre-differentiated MSCs. Only by day 16 of culture for the PCL/ECM constructs does the spectrum start to resemble that of mature bone.

However, the nodules on the surface of the constructs seen in Figure 2 do not resemble the mineralized surface of mature bone. Mature bone is known to have a highly ordered surface composed of plate-like crystals of nano-crystalline HAp with many ion substitutes. 41,43–45 Even the longest culture period constructs, PCL day 16 and PCL/ECM day 16, which have some nodules that look needle-like, do not resemble mature bone (SEM micrograph not shown). Nevertheless, the surface of the constructs may change at a later point, due to the crystals growing larger and fusing together or through an organization of the ECM.

Conclusions

Overall, this study demonstrates that MSCs seeded upon PCL-based constructs and cultured under engineered conditions with a flow perfusion bioreactor deposit cell adhesive, structural, remodeling, and regulatory proteins as well as hydroxyapatite minerals found in developing and mature bone. The protein composition of the constructs as they are cultured over time revealed that the MSCs deposited cellular adhesion proteins, such as fibronectin, at short culture durations, while they deposited matrix remodeling and regulatory proteins, such as MMP-2 and PEDF, at long culture durations. The constructs were seen to contain the major components of mature bone, collagen 1 and hydroxyapatite. The constructs also contain fibril-regulating proteins that help to organize collagen 1 and fibronectin, and matrix remodeling proteins, thus the ECM has started to resemble that of mature bone. However, only one anti-angiogenic growth factor and no glycosaminoglycan-substituted proteoglycans were identified. Further analysis will be needed to determine the effect that ECM maturity has on bone formation and regeneration *in vivo*.

Acknowledgments

This work was supported by a grant from the National Institutes of Health (R01 AR057083), a grant from the Bioengineering Research Partnership with the Baylor College of Medicine through the National Institute of Biomedical Imaging and Bioengineering (R01 EB005173), and a Ruth L. Kirschstein National Research Service Award (F31 AR055874) from the National Institute of Arthritis and Musculoskeletal and Skin Diseases. The content is solely the responsibility of the authors and does not necessarily represent the official views of the National Institute of Arthritis and Musculoskeletal and Skin Diseases or the National Institutes of Health.

References

- 1. Burstein FD. Cleft Palate Craniofac. J. 2000; 37:1-4. [PubMed: 10670881]
- 2. Artico M, Ferrante L, Pastore FS, Ramundo EO, Cantarelli D, Scopelliti D, Iannetti G. Surg. Neurol. 2003; 60:71–79. [PubMed: 12865021]
- 3. Banwart JC, Asher MA, Hassanein RS. Spine. 1995; 20:1055–1060. [PubMed: 7631235]
- Skaggs DL, Samuelson MA, Hale JM, Kay RM, Tolo VT. Spine. 2000; 25:2400–2402. [PubMed: 10984795]
- Bilezikian, JP.; Raisz, LG.; Rodan, GA. Principles of Bone Biology. 2nd ed. San Diego: Academic Press; 2002.
- 6. Chen G, Ushida T, Tateishi T. J. Biomed. Mater. Res. 2001; 57:8-14. [PubMed: 11416843]
- Habraken WJ, Boerman OC, Wolke JG, Mikos AG, Jansen JA. J. Biomed. Mater. Res. A. 2009; 91:614–622. [PubMed: 18985784]
- 8. Ratanavaraporn J, Furuya H, Kohara H, Tabata Y. Biomaterials. 2011; 32:2797–2811. [PubMed: 21257197]
- 9. Patel ZS, Yamamoto M, Ueda H, Tabata Y, Mikos AG. Acta Biomater. 2008; 4:1126–1138. [PubMed: 18474452]
- Patel ZS, Young S, Tabata Y, Jansen JA, Wong ME, Mikos AG. Bone. 2008; 43:931–940.
 [PubMed: 18675385]
- Liao J, Guo X, Nelson D, Kasper FK, Mikos AG. Acta Biomater. 2010; 6:2386–2393. [PubMed: 20080214]
- Thibault RA, Baggett LS, Mikos AG, Kasper FK. Tissue Eng. Part A. 2009; 16:431–440.
 [PubMed: 19863274]
- Datta N, Pham QP, Sharma U, Sikavitsas VI, Jansen JA, Mikos AG. Proc. Natl. Acad. Sci. 2006; 103:2488–2493. [PubMed: 16477044]
- 14. Pham QP, Kasper FK, Baggett LS, Raphael RM, Jansen JA, Mikos AG. Biomaterials. 2008; 29:2729–2739. [PubMed: 18367245]
- 15. Pham QP, Sharma U, Mikos AG. Biomacromolecules. 2006; 7:2796–2805. [PubMed: 17025355]
- Holtorf HL, Jansen JA, Mikos AG. J. Biomed. Mater. Res. A. 2005; 72:326–334. [PubMed: 15657936]
- 17. Bancroft GN, Sikavitsas VI, Mikos AG. Tissue Eng. 2003; 9:549-554. [PubMed: 12857422]
- Perkins DN, Pappin DJ, Creasy DM, Cottrell JS. Electrophoresis. 1999; 20:3551–3567. [PubMed: 10612281]
- 19. Ishihama Y, Oda Y, Tabata T, Sato T, Nagasu T, Rappsilber J, Mann M. Mol. Cell Proteomics. 2005; 4:1265–1272. [PubMed: 15958392]
- 20. Singh P, Carraher C, Schwarzbauer JE. Annu. Rev. Cell Dev. Biol. 2010; 26:397–419. [PubMed: 20690820]
- Sabatelli P, Bonaldo P, Lattanzi G, Braghetta P, Bergamin N, Capanni C, Mattioli E, Columbaro M, Ognibene A, Pepe G, Bertini E, Merlini L, Maraldi NM, Squarzoni S. Matrix Biol. 2001; 20:475–486. [PubMed: 11691587]
- Maruhashi T, Kii I, Saito M, Kudo A. J. Biol. Chem. 2010; 285:13294–13303. [PubMed: 20181949]
- 23. Itoh T, Tanioka M, Yoshida H, Yoshioka T, Nishimoto H, Itohara S. Cancer Res. 1998; 58:1048–1051. [PubMed: 9500469]
- Argraves WS, Tran H, Burgess WH, Dickerson K. J. Cell Biol. 1990; 111:3155–3164. [PubMed: 2269669]
- 25. Canfield AE, Hadfield KD, Rock CF, Wylie EC, Wilkinson FL. Biochem. Soc. Trans. 2007; 35:669–671. [PubMed: 17635117]
- 26. Zhang X, Lawler J. Microvasc. Res. 2007; 74:90–99. [PubMed: 17559888]
- Tombran-Tink J, Barnstable CJ. Biochem. Biophys. Res. Commun. 2004; 316:573–579. [PubMed: 15020256]
- 28. Kazerounian S, Yee KO, Lawler J. Cell Mol.Life Sci. 2008; 65:700–712. [PubMed: 18193162]

- 29. McKee MD, Nanci A. Microsc. Res. Tech. 1996; 33:141-164. [PubMed: 8845514]
- 30. Brochmann EJ, Behnam K, Murray SS. Metabolism. 2009; 58:644–650. [PubMed: 19375587]
- 31. Orimo HJ. Nippon Med. Sch. 2010; 77:4–12.
- 32. Kozaki K, Miyaishi O, Koiwai O, Yasui Y, Kashiwai A, Nishikawa Y, Shimizu S, Saga S. J. Biol. Chem. 1998; 273:15125–15130. [PubMed: 9614124]
- 33. Quan GM, Ojaimi J, Li Y, Kartsogiannis V, Zhou H, Choong PF. Calcif. Tissue Int. 2005; 76:146–153. [PubMed: 15549636]
- 34. Hankenson KD, Sweetwyne MT, Shitaye H, Posey KL. Curr. Osteoporos. Rep. 2010; 8:68–76. [PubMed: 20425613]
- 35. Dai J, Rabie AB. J. Dent. Res. 2007; 86:937-950. [PubMed: 17890669]
- 36. Park MS, Kim SS, Cho SW, Choi CY, Kim BS. J. Biomed. Mater. Res. B Appl. Biomater. 2006; 79:353–359. [PubMed: 16924630]
- 37. Miao HQ, Ishai-Michaeli R, Atzmon R, Peretz T, Vlodavsky I. J. Biol. Chem. 1996; 271:4879–4886. [PubMed: 8617759]
- 38. Jansen JA, Vehof JW, Ruhé PQ, Kroeze-Deutman H, Kuboki Y, Takita H, Hedberg EL, Mikos AG, J. Control Release. 2005; 101:127–136. [PubMed: 15588899]
- 39. Gomes ME, Bossano CM, Johnston CM, Reis RL, Mikos AG. Tissue Eng. 2006; 12:177–188. [PubMed: 16499454]
- 40. Holtorf HL, Datta N, Jansen JA, Mikos AG. J. Biomed. Mater. Res. A. 2005; 74:171–180. [PubMed: 15965910]
- 41. LeGeros RZ. Chem. Rev. 2008; 108:4742–4753. [PubMed: 19006399]
- 42. Boskey AL. J. Dent. Res. 1997; 76:1433–1436. [PubMed: 9240379]
- 43. Weiner S, Wagner HD. Ann. Rev. Mater. Sci. 1998; 28:271-298.
- 44. Boskey AL. Osteoporos. Int. 2003; 14 Suppl 5:S16–S20. discussion S20-11. [PubMed: 14504701]
- 45. Palmer LC, Newcomb CJ, Kaltz SR, Spoerke ED, Stupp SI. Chem. Rev. 2008; 108:4754–4783. [PubMed: 19006400]

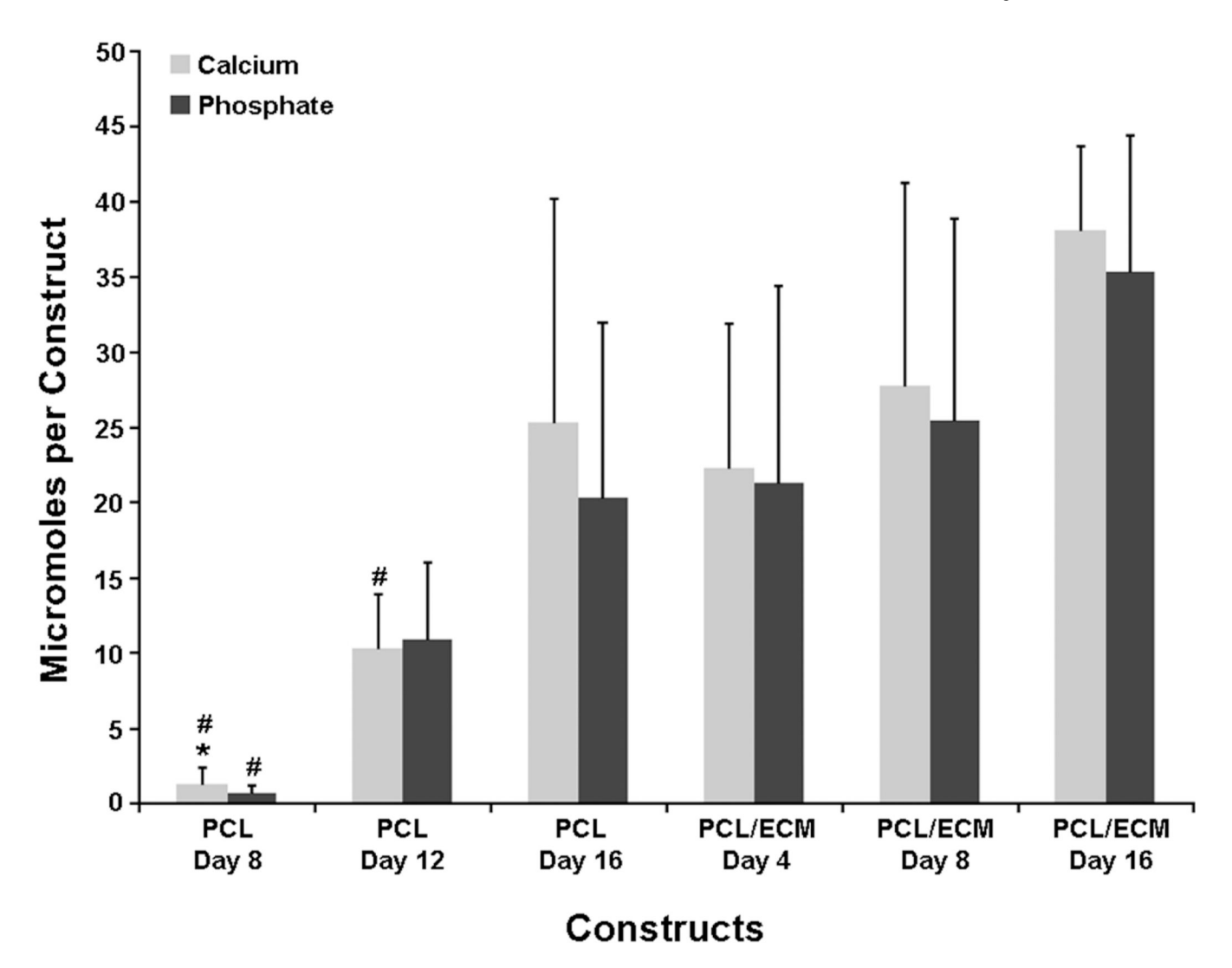


Figure 1. The amount of calcium and phosphate ions present in each scaffold at different stages of the ECM maturity. The * symbol represents a significant difference of p<0.05 to the PCL/ECM day 8 group and the # symbol represents a significant difference of p<0.05 to the PCL/ECM day 16 group. Data are expressed as means \pm standard deviation for n=3.

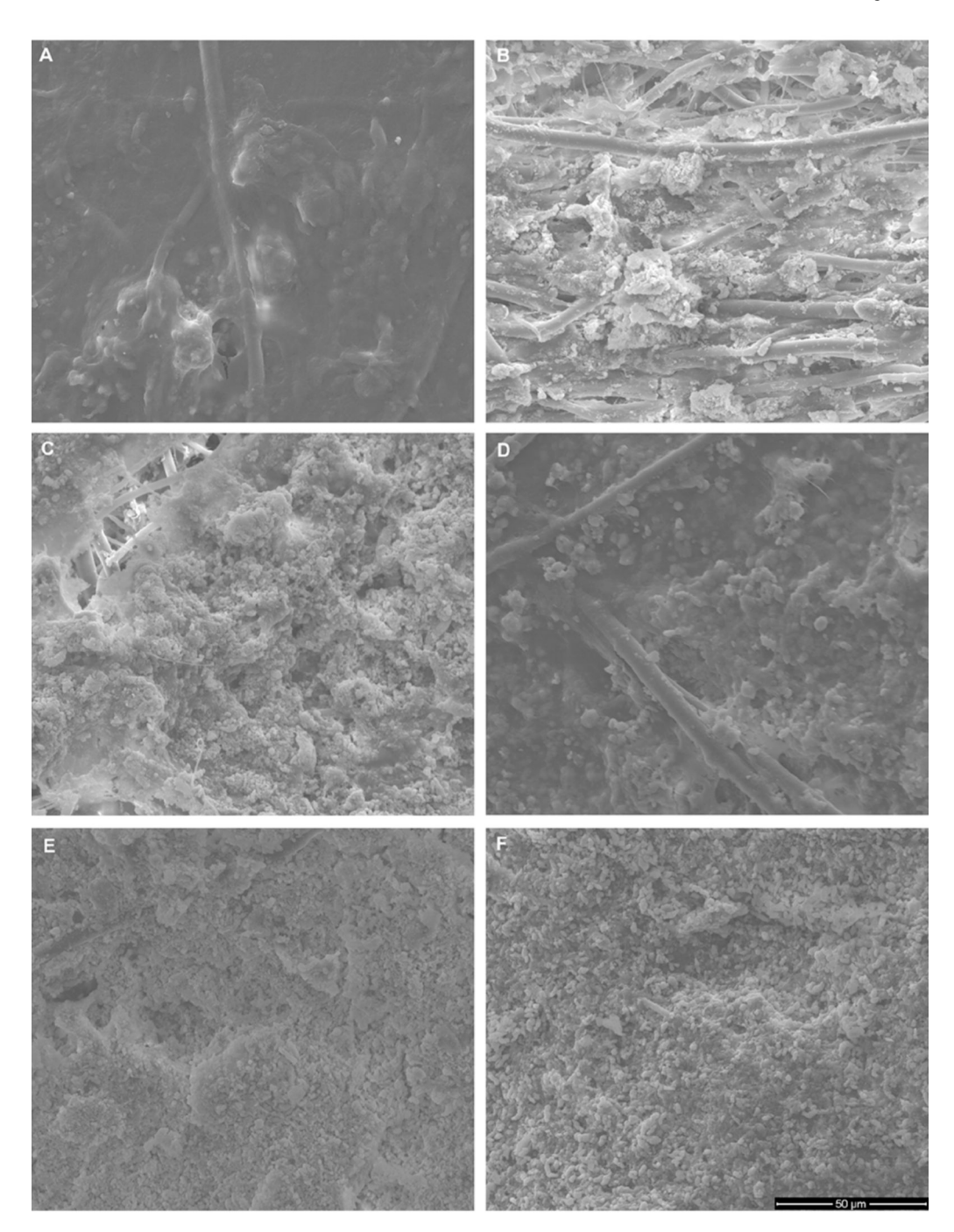


Figure 2.SEM micrographs of the top of the flow generated acellular constructs. A) PCL day 8, B) PCL day 12, C) PCL day 16, D) PCL/ECM day 4, E) PCL/ECM day 8, F) PCL/ECM day 16. As culture duration increases, there is an appearance and growth of mineral nodules on the surface.

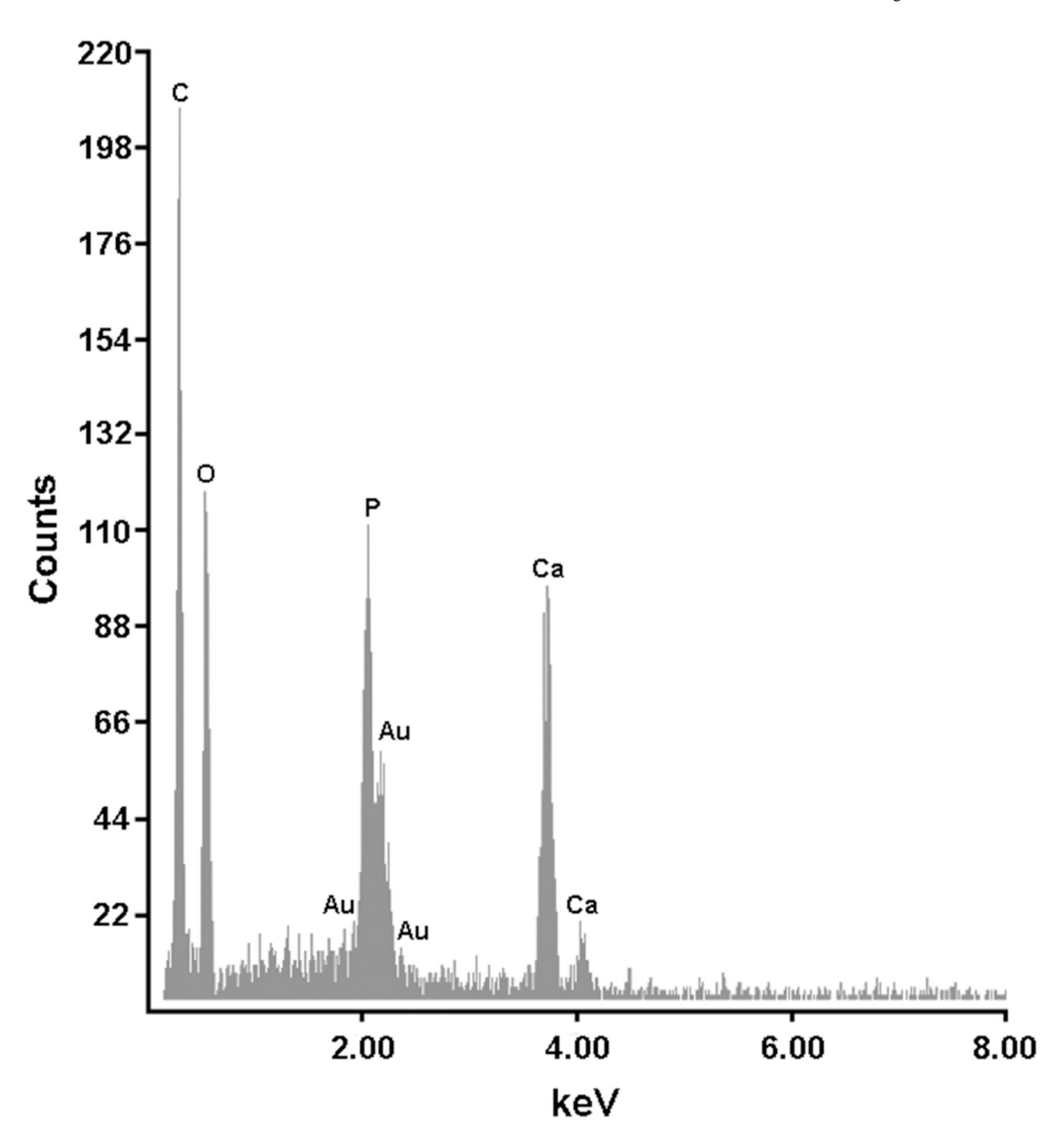


Figure 3. A representative EDX spectrum of the constructs. EDX analysis demonstrates the presence of carbon, oxygen, calcium, phosphorous, and gold on the surface of the constructs. The presence of gold is due to its use in coating the constructs for SEM imaging.

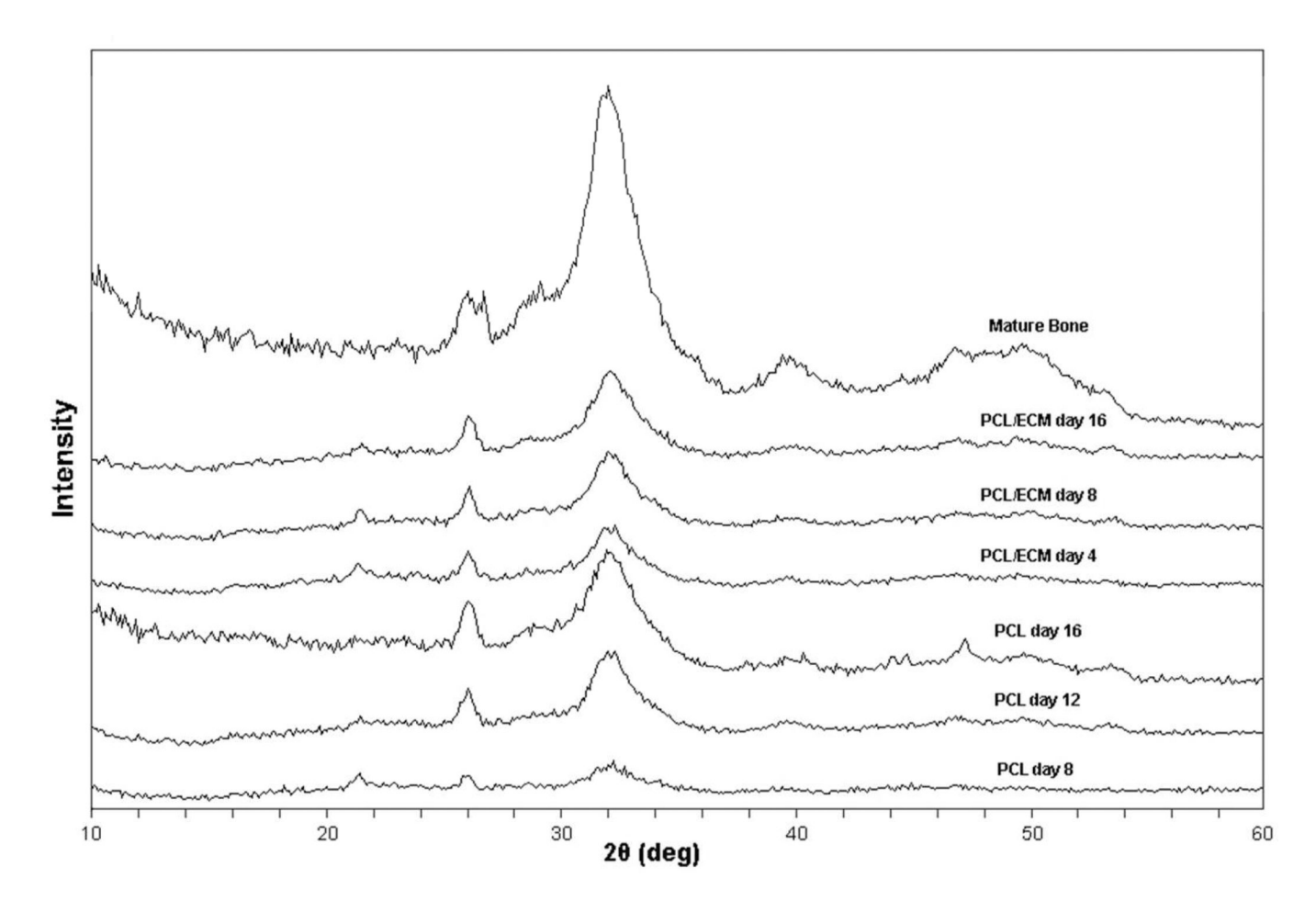


Figure 4. XRD spectra of the constructs. The PCL day 8 construct demonstrates minor broad peaks within the scan range. All other constructs demonstrate broad peaks at 26° and 32° . Peaks at 28° , 40° , and 50° can be seen in PCL day 16 and PCL/ECM day 16 constructs, similar to those seen in mature bone.

Table 1

ECM Protein Analysis by LC-MS/MS

The proteins present within each type of construct as found by LC-MS/MS. The best match for each protein and the associated Mascot score are

Thibault et al.

PCL day 8 PCL day 12 PCL day 12	Access ion.Version (NCBInr)	Protein	Mass (Da)	Mascot Score	No. of Unique Peptides	emPAI
CL day 12 CL day 12	N/A	None Detected	N/A	N/A	N/A	N/A
CL day 12	EDL75262.1	Fibronectin 1, isoform CRA-d (FN1)	262747	604	12	0.21
!	EDM14936.1	Periostin, osteoblast specific factor (predicted), isoform CRA_d (Postn)	90251	199	4	0.09
PCL day 12	EDL92064.1	Procollagen, type VI, $\alpha 3$ (predicted), isoform CRA_d (Col6)	233804	166	4	0.05
PCL day 12	CAB01633.1	Collagen al, type 1 (Col1)	137885	94	2	90.0
PCL day 12	CAA50583.1	Type IV collagenase (MMP-2)	74181	82	1	90.0
PCL day 12	NP_001121019.1	Fibulin-1 (FBLN1)	78071	89	2	None
PCL day 16	EDL75262.1	Fibronectin 1, isoform CRA_d (FN1)	262747	616	12	0.17
PCL day 16	EDL92061.1	Procollagen, type VI, $\alpha 3$ (predicted), isoform CRA_b (Col6)	311351	124	к	0.03
PCL day 16	CAB01633.1	Collagen a1, type 1 (Coll)	132885	105	2	90.0
PCL day 16	EDM14936.1	Periostin, osteoblast specific factor (predicted), isoform CRA_d (Postn)	90251	93	7	0.05
PCL day 16	CAA50583.1	Type IV collagenase (MMP-2)	74181	71	1	90.0
PCL day 16	NP_001162609.1	Thrombospondin 2 precursor (TSP-2)	129726	65	2	None
PCL day 16	NP_113909.1	HtrA serine peptidase 1 (HtrA1)	51330	63	1	0.08
PCL day 16	NP_808788.1	Pigment epithelium-derived factor (PEDF)	46465	51	1	0.09
PCL/ECM 0	PO4937.2	Fibronectin 1 (FN1)	272341	99	2	0.03
PCL/ECM 0	NP_001121019.1	Fibulin-1 (FBLN1)	78019	61	2	0.10
PCL/ECM 0	NP_113909.1	HtrA serine peptidase 1 (HtrA1)	51298	59	8	0.23
PCL/ECM 0	CAB01633.1	Collagen al, type 1 (Col1)	137802	48	8	0.05
PCL/ECM 0	NP_001013080.1	Thrombospondin 1 (TSP-1)	129588	39	1	0.03
PCL/ECM 0	EDL97133.1	Procollagen, type VI, α1 (predicted)	75928	32	1	0.05

Page 17

Construct	Access ion.Version (NCBInr)	Protein	Mass (Da)	Mascot Score	Mass (Da) Mascot No. of Unique Score Peptides	emPAI
PCL/ECM day 4	AAA87903.1	Secreted phosphoprotein-24 precursor (SPP-24/SPP-2)	20687	73	1	0.21
PCL/ECM day 8	EDL92061.1	Procollagen, type VI, a.3 (predicted), isoform CRA_b (Col6)	311351	49	1	0.01
PCL/ECM day 8	EDM14934.1	Periostin, osteoblast specific factor (predicted), isoform CRA_b (Postn)	77695	43	-	0.05
PCL/ECM day 16	EDL92063.1	Procollagen, type VI, $\alpha 3$ (predicted), isoform CRA_d (Col6)	233804	808	12	0.23
PCL/ECM day 16	NP_001121019.1	Fibulin-1 (FBLN1)	78071	91	2	0.11
PCL/ECM day 16	EDL75260.1	Fibronectin 1, isoform CRA-b (FN1)	253107	78	2	0.03
PCL/ECM day 16	CAA68703.1	Alkaline phosphatase (ALP)	57810	99	2	0.07
PCL/ECM day 16	NP 808788.1	Pigment epithelium-derived factor (PEDF)	46465	51	1	0.00

Thibault et al.

Page 18

Table 2

Calcium to Phosphorous Ratio

The ratio of calcium to phosphorous present on the constructs as determined by the calcium and phosphate assays and by EDX analysis. The Ca:P ratio is indicative of the type of calcium phosphate present, with pure hydroxyapatite having a Ca:P ratio of 1.67. Data are expressed as means \pm standard deviation for n=3 for the Ca and PO₄ assay. EDX data are expressed as means \pm standard deviation for three separate spots analyzed on a single sample.

Construct	Ca & PO ₄ Assay Ca:P ratio	EDX Ca:P ratio	
PCL day 8	1.47 ± 0.52	1.12 ± 0.05	
PCL day 12	1.02 ± 0.29	1.45 ± 0.13	
PCL day 16	1.24 ± 0.09	1.51 ± 0.07	
PC:/ECM day 4	1.14 ± 0.21	1.36 ± 0.05	
PCL/ECM day 8	1.09 ± 0.14	1.62 ± 0.02	
PCL/ECM day 16	1.10 ± 0.15	1.53 ± 0.04	
Mature Bone	1.99 ± 0.11	1.41 ± 0.02	

Table 3 Crystallinity and Mineral Composition by XRD

The crystallinity and figure of merit for the fit of each mineral type present as determined by XRD. The 2θ offset represents the shift (in degrees) required by the software to match the respective spectra to the HAp or TCP peaks within the PDF 4 database. The (M) represents a major phase and the (m) represents a minor phase. Data are expressed as means \pm standard deviation for three manual fittings of the spectra obtained from a single sample comprising the combined mineral component of six constructs.

Construct	Crystallinity	Mineral	Figure of Merit	2θ offset
PCL day 8	N/A	N/A	N/A	N/A
PCL day 12	82.12 ± 6.58%	Hydroxyapatite (M)	41.3	0.000
		Tricalcium Phosphate (m)	25.1	0.060
PCL day 16	89.10 ± 0.75%	Hydroxyapatite (M)	11.7	0.080
		Tricalcium Phosphate (m)	10.9	0.080
PCL/ECM day 4	82.54 ± 3.64%	Hydroxyapatite (M)	33.8	0.000
		Tricalcium Phosphate (m)	23.3	-0.060
PCL/ECM day 8	80.05 ± 6.92%	Hydroxyapatite (M)	24.3	0.100
		Tricalcium Phosphate (m)	28.3	0.000
PCL/ECM day 16	85.91 ± 10.11%	Hydroxyapatite (M)	28.4	0.040
		Tricalcium Phosphate (m)	29.5	0.080
Mature Bone	84.39 ± 1.23%	Hydroxyapatite (M)	25.2	0.000
		Tricalcium Phosphate (m)	18.4	-0.020